



This is a repository copy of *Origin of solvent-induced polymorphism in self-assembly of trimesic acid monolayers at solid-liquid interfaces*.

White Rose Research Online URL for this paper:
<https://eprints.whiterose.ac.uk/160228/>

Version: Supplemental Material

Article:

Ochs, O., Hocke, M., Spitzer, S. et al. (3 more authors) (2020) Origin of solvent-induced polymorphism in self-assembly of trimesic acid monolayers at solid-liquid interfaces. *Chemistry of Materials*, 32 (12). pp. 5057-5065. ISSN 0897-4756

<https://doi.org/10.1021/acs.chemmater.0c00827>

This document is the Accepted Manuscript version of a Published Work that appeared in final form in *Chemistry of Materials*, copyright © American Chemical Society after peer review and technical editing by the publisher. To access the final edited and published work see <https://doi.org/10.1021/acs.chemmater.0c00827>.

Reuse

Items deposited in White Rose Research Online are protected by copyright, with all rights reserved unless indicated otherwise. They may be downloaded and/or printed for private study, or other acts as permitted by national copyright laws. The publisher or other rights holders may allow further reproduction and re-use of the full text version. This is indicated by the licence information on the White Rose Research Online record for the item.

Takedown

If you consider content in White Rose Research Online to be in breach of UK law, please notify us by emailing eprints@whiterose.ac.uk including the URL of the record and the reason for the withdrawal request.



eprints@whiterose.ac.uk
<https://eprints.whiterose.ac.uk/>

Supporting Information

Origin of Solvent-Induced Polymorphism in Self-Assembly of Trimesic Acid Monolayers at Solid-Liquid Interfaces

Oliver Ochs[†], Manuela Hocke[†], Saskia Spitzer[†], Wolfgang M. Heckl[†], Natalia Martsinovich[‡], and Markus Lackinger^{†}*

[†]Department of Physics, Technische Universität München, James-Franck-Str. 1, 85748 Garching, Germany; Deutsches Museum, Museumsinsel 1, 80538 Munich, Germany;

[‡]Department of Chemistry, University of Sheffield, Sheffield S3 7HF, UK;

Experimental determination of TMA sublimation enthalpy ΔH_{sub}

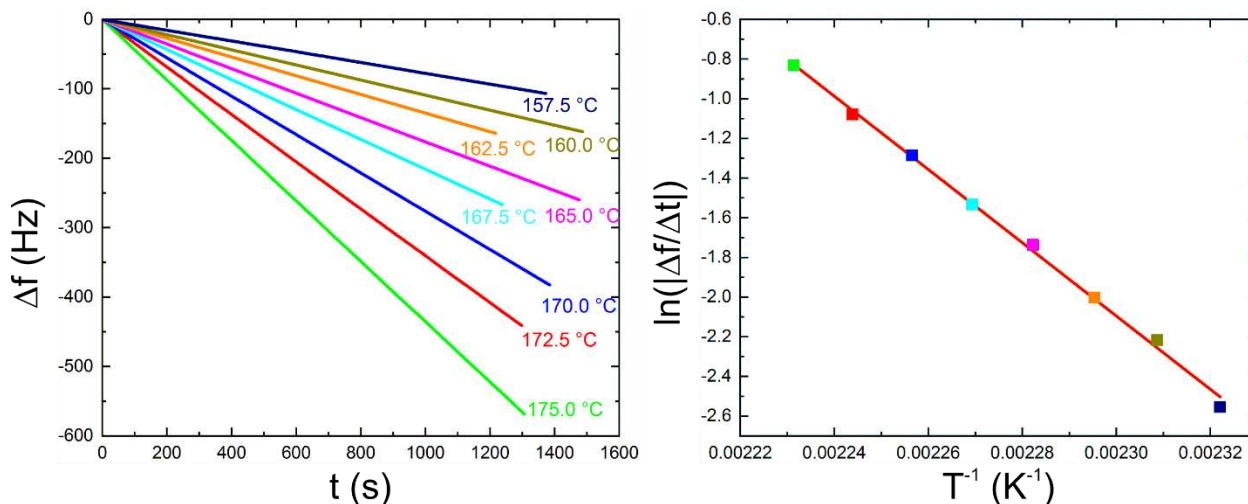


Figure S1. The TMA sublimation enthalpy ΔH_{sub} was determined from indirect measurements of the TMA saturated vapor pressure as a function of temperature in effusion experiments using a home-built Knudsen cell and a water-cooled Quartz Crystal Microbalance (QCMB).¹ (a) Change of the QCMB resonant frequency Δf versus time t traces for the indicated crucible temperatures of the Knudsen cell. Slopes of individual traces (corresponding to deposition rates) were obtained from linear fits. (b) Corresponding Van't Hoff plot of deposition rates and crucible temperatures. The red line represents a linear fit to the individual data points and from its slope a TMA sublimation enthalpy of $\Delta H_{sub} = 154 \frac{\text{kJ}}{\text{mol}}$ is deduced. The perfectly linear behavior indicates a negligible temperature dependence of ΔH_{sub} in this temperature range.

UV-Vis absorption spectra

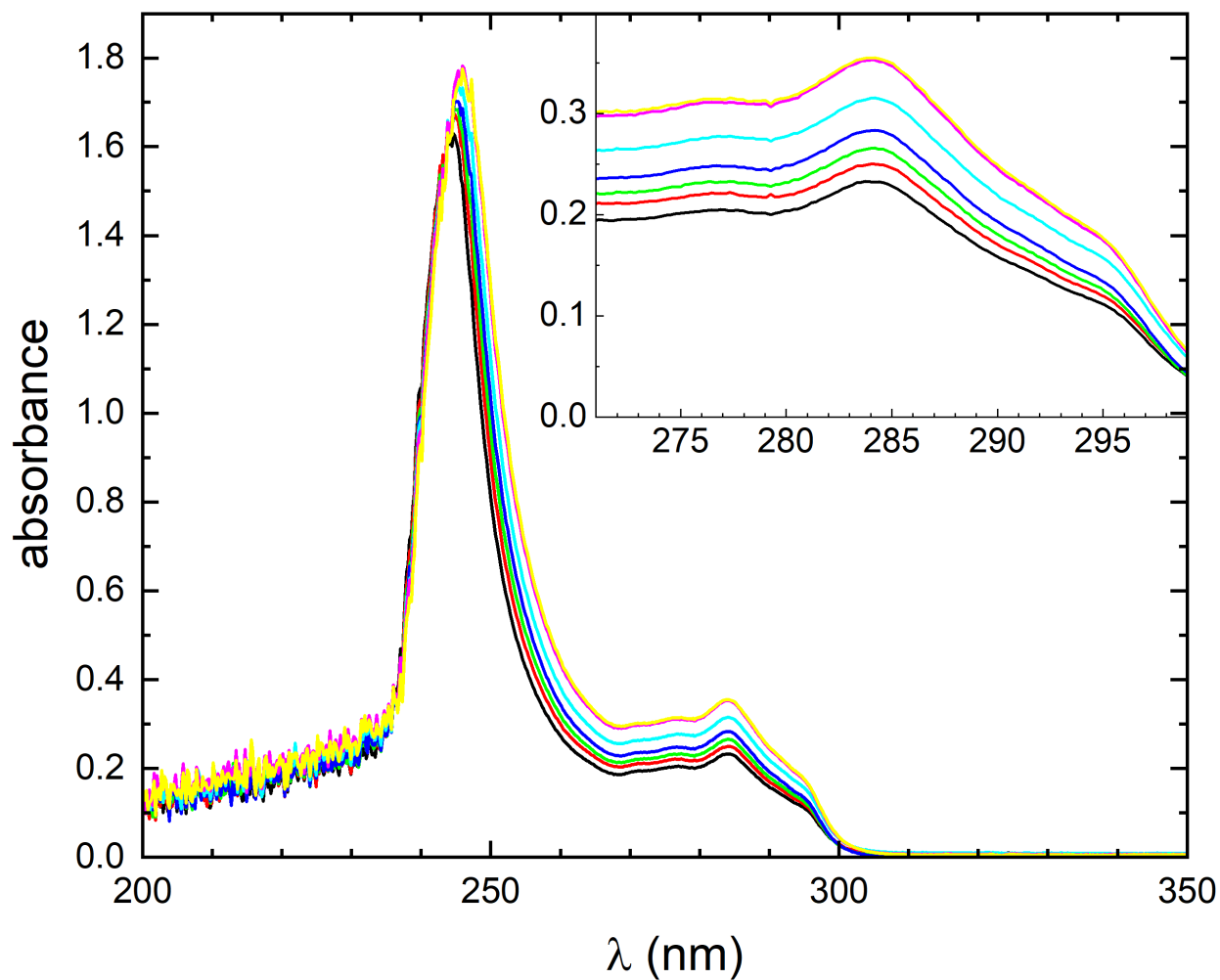


Figure S2. UV-Vis absorption spectra of saturated TMA in 6A solutions acquired for temperatures from 30.0 °C (black curve at the bottom) to 60 °C with temperature increments of 5.0 °C. The increasing absorbance for increasing temperature indicates an endothermic dissolution. For the Van't Hoff plot (cf. Figure 2 of the main manuscript) the absorbance was integrated in the spectral range $\lambda = (281 - 287) \text{ nm}$, i.e. in a region where the absorbance is reasonably low to provide reliable values.

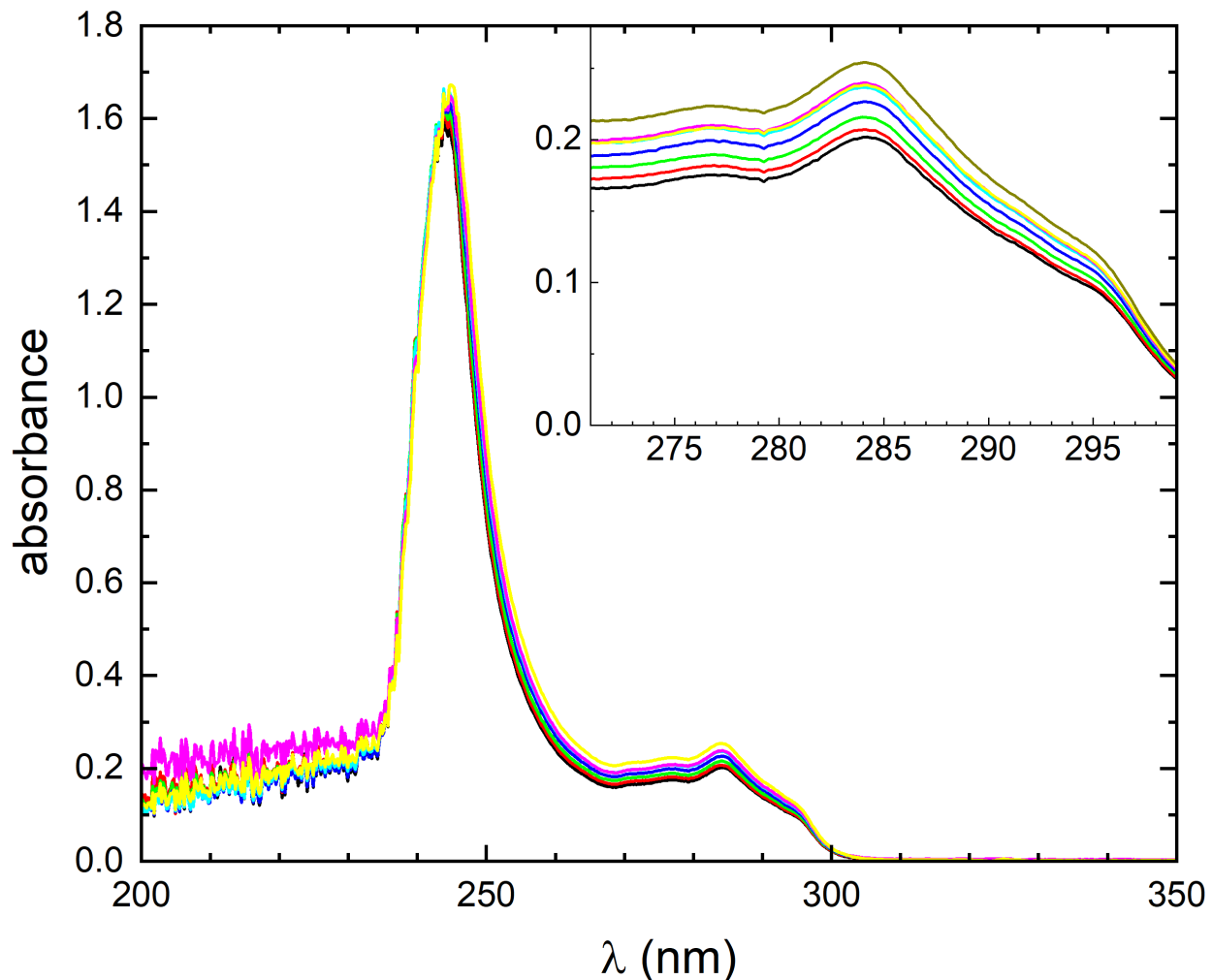


Figure S3. UV-Vis absorption spectra of saturated TMA in 7A solutions acquired for temperatures from 32.5 °C (black curve at the bottom) to 50.0 °C with temperature increments of 2.5 °C. To exclude systematic errors due to for instance kinetic effects, temperatures were varied non monotonously. The increasing absorbance for increasing temperature indicates an endothermic dissolution. For the Van't Hoff plot (cf. Figure 2 of the main manuscript) the absorbance was integrated in the spectral range $\lambda = (281 - 287) \text{ nm}$, i.e. in a region where the absorbance is reasonably low to provide reliable values.

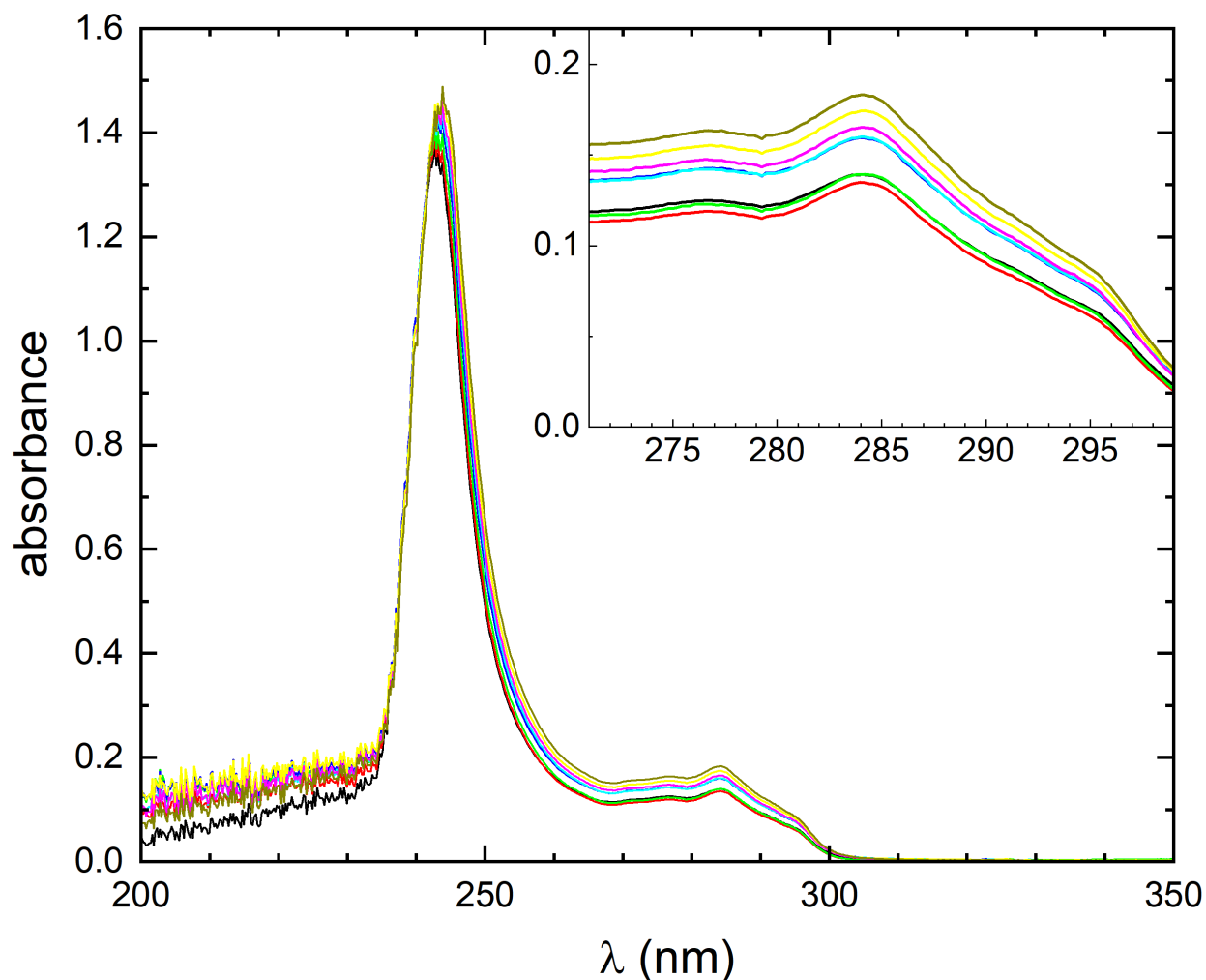


Figure S4. UV-Vis absorption spectra of saturated TMA in 9A solutions acquired for temperatures from 32.5 °C (black curve at the bottom) to 50.0 °C with temperature increments of 2.5 °C. To exclude systematic errors due to for instance kinetic effects, temperatures were varied non monotonously. The increasing absorbance for increasing temperature indicates an endothermic dissolution. For the Van't Hoff plot (cf. Figure 2 of the main manuscript) the absorbance was integrated in the spectral range $\lambda = (281 - 287) \text{ nm}$, i.e. in a region where the absorbance is reasonably low to provide reliable values.

Additional STM data

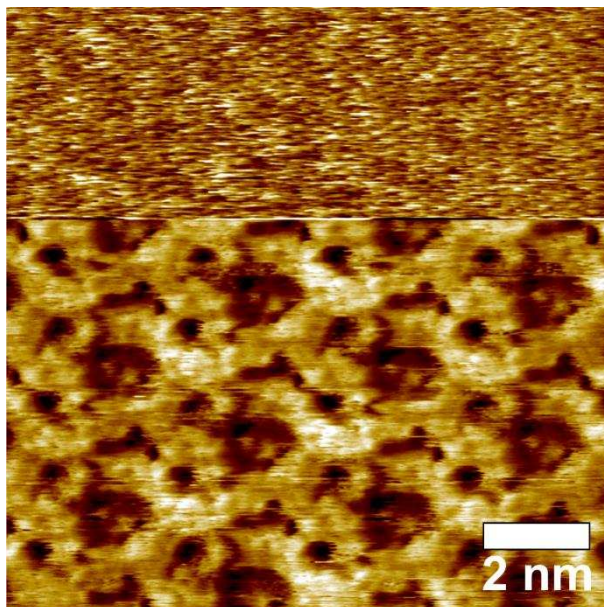


Figure S5. STM image of the TMA flower polymorph on graphite(0001) acquired in saturated 6A solution. The lower part of this “split-image” shows the molecular structure, whereas after reducing the tunneling voltage the underlying graphite substrate was imaged in the upper part. From this and other comparable images an angle of $\alpha = 5.5^\circ \pm 1.0^\circ$ between the lattices of the TMA flower polymorph and graphite was extracted. From STM images experimental lattice parameters of $a = b = (2.60 \pm 0.05) \text{ nm}$ were derived for the TMA flower polymorph. These experimental data are in perfect agreement with the proposed $\begin{pmatrix} 11 & 1 \\ -1 & 10 \end{pmatrix}$ commensurate superstructure as used for the DFT simulations (*vide supra*), resulting in $\alpha_{\text{commensurate}} = 4.7^\circ$ and $a_{\text{commensurate}} = b_{\text{commensurate}} = 2.59 \text{ nm}$. (sample voltage used for imaging TMA and current setpoint: -588 mV, 62.4 pA).

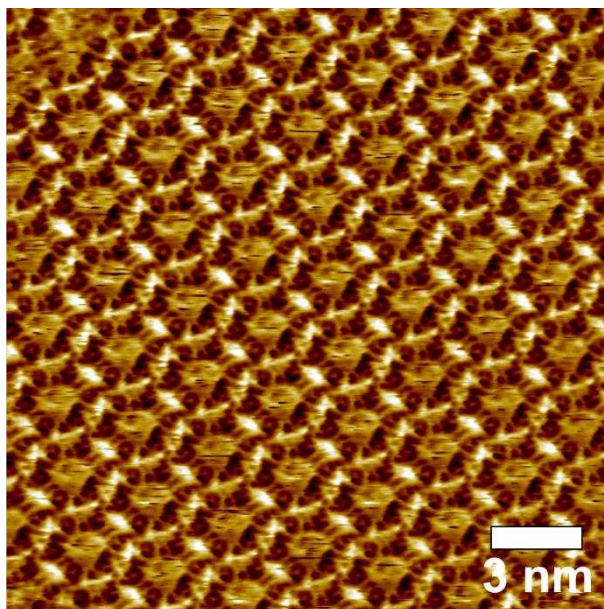


Figure S6. STM image of the TMA flower polymorph on graphite(0001) acquired in saturated 6A solution. In the STM contrast of this image both types of pores appear brighter than the TMA networks. This inverted contrast is frequently observed for the flower polymorph in 6A and provides further evidence for solvent co-adsorption in both types of pores, i.e. the smaller elongated and the larger circular pores (sample voltage and current setpoint: -600 mV, 53 pA).

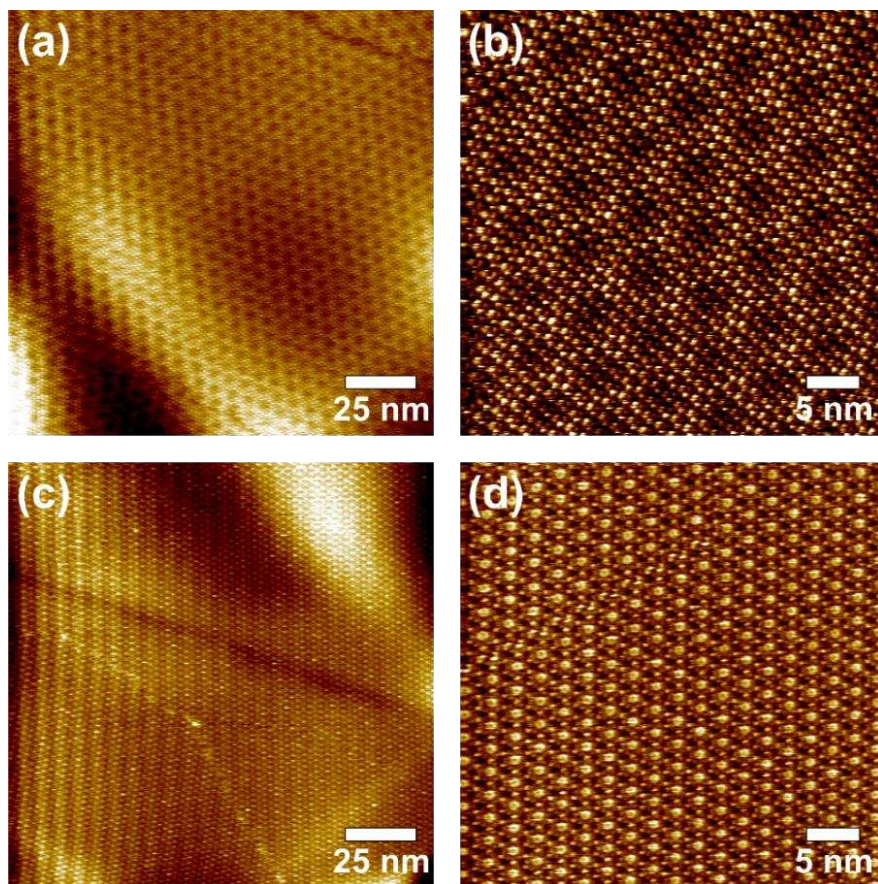


Figure S7. STM images of TMA monolayers acquired (a) / (b) after initially applying saturated TMA in 7A solution onto graphite(0001) and (c) / (d) after additionally applying an excess of saturated TMA in 6A solution. After applying the 7A solution the entire surface was covered with the chickenwire polymorph as anticipated. In large scale images the chickenwire polymorph can be immediately identified by its characteristic Moiré pattern.² After applying an excess of saturated 6A solution the entire sample was covered with the flower polymorph. Various different sample areas were probed by STM without observing any remains of the chickenwire polymorph. The spontaneous transformation of the chickenwire into the flower polymorph already at room temperature after changing the solvent from 7A to 6A indicates both higher thermodynamical stability of the flower polymorph in 6A and the absence of kinetic trapping (sample voltages and current setpoints: (a) / (b) +690 mV, 50.9 pA; (c) / (d) +590 mV, 56.3 pA).

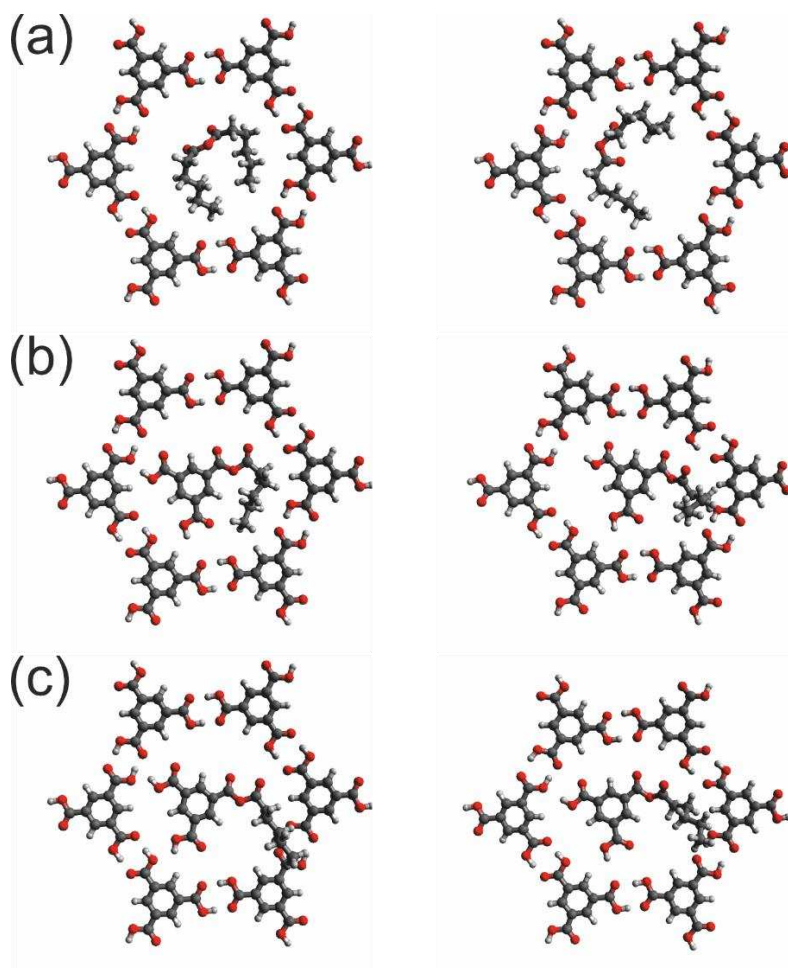


Figure S8. DFT-optimization and Molecular Dynamics (MD) simulations of different TMA and hexanoic acid (6A) anhydrides as possible guest-species in the ~ 1 nm wide circular pore that is common to both flower and chickenwire polymorph. The left hand sides show the outcomes of structure optimization, whereas the structures obtained after 1 ps long MD runs are shown on the right hand sides. Calculations were performed on graphene (omitted for clarity). (a) 6A anhydride (-1.25 eV); (b) TMA 6A anhydride species with initially flat adsorbed alkane tails (-1.55 eV); (c) TMA 6A anhydride species with initially upright adsorbed alkane tails (-1.43 eV); Although the influence of the supernatant solution is neglected here, the respective binding energies (stated in parenthesis) are reasonably large to conclude on stable adsorption of these species within the pores.

References

1. Gutzler, R.; Heckl, W. M.; Lackinger, M., Combination of a Knudsen effusion cell with a quartz crystal microbalance: in-situ measurement of molecular evaporation rates with a fully functional deposition source. *Rev Sci Instrum* **2009**, *81*, 015108.
2. Spitzer, S.; Helmle, O.; Ochs, O.; Horsley, J.; Martsinovich, N.; Heckl, W. M.; Lackinger, M., What can be inferred from moire patterns? A case study of trimesic acid monolayers on graphite. *Faraday Discuss.* **2017**, *204*, 331-348.